Part I

Fluid Dynamics

Franz Durst

Institute of Fluid Mechanics
Friedrich-Alexander-Universität Erlangen-Nürnberg
Cauerstr. 4
91058 Erlangen, Germany

Computational Fluid Mechanics is one of the subjects that benefited considerably from support received through KONWIHR to apply high performance computer codes on large computers to study fluid flows and related problems. The success of seven of the projects was impressively demonstrated by the presentations of results obtained. In this section, the written versions of the project presentations are given to complete the information already made available at the closing colloquium of KONWIHR in Munich on the 14th and 15th October 2004.

BESTWIHR was a project within KONWIHR that aimed at the application of the developed computer code BEST to numerically predict turbulent channel flows. Most DNS-predictions were carried out in the past using spectral methods or finite-volume techniques; the aim within the BESTWIHR-project was to utilize the Lattice-Boltzmann techniques for direct numerical simulations of turbulent channel flows. Results obtained are summarised in the first paper in this section. A good agreement is shown with existing data for the mean velocity profile, the turbulence intensity distribution and also some higher-order moments. Only the higher-order moments of the v-component (perpendicular to the wall) show the same defect as predicted with other methods.

The project DiSiVGT was set up within KONWIHR in order to utilise data from direct numerical simulations obtained within the project and also within BESTWIHR for verifying the assumptions introduced into statistical turbulence models. The work took into account that the development of turbulence closure for flow predictions was heavily limited by the lack of adequate data. For nearly all important quantities which are required in the application of the closure assumptions, experimental measurements are difficult, or sometimes even impossible. With the appearance of direct numerical simulations, significant progress has been made in this respect by exploring numerical databases. These databases contain the complete budgets of all important quantities which are necessary for the direct verification of the closure assumptions currently employed. New directions in turbulence research closely follow computer technology, which is in an advanced stage of development.

Some of the new fundamental contributions to understanding turbulence phenomena have been obtained by exploring these databases. Furthermore, new modelling concepts based on the anisotropy invariants were evaluated with these DNS data.

FlowNoise is the third paper in this section. It describes how the computer code FASTEST-3D was used for large-eddy simulations in order to obtain the source terms for the noise production in fluid flows. FASTEST-3D was coupled with a program called CFS++ to predict flow induced in noise. The data were analyzed to understand physically how noise is produced. In KONWIHR all the work could be done to run both programs efficiently on supercomputers. FlowNoise will provide the basis for efficient studies of sources of noise in technical equipment.

FLUSIB was a project within KONWIHR that studied the coupling of fluid flows within thin-walled structures. Structural simulations were carried out using three-dimensional higher-order elements and the flow computations were performed with finite-volume methods using the large eddy simulation approach. Special attention was given to effective coupling of the structural and fluid information in order to maintain the efficiency of both programs in the combined fluid flow and structural computations. Finally, several technical applications were considered, e.g. the wind-excitation of a thin-walled tower.

Within RexSim simulations were carried out to incorporate efficiently the computation of combined radiative and conductive heat transfer into numerical computer codes. Monte-Carlo simulations were carried out and a specially formulated solution method was employed to avoid the time consuming rate raising part of the Monte-Carlo method. Efficiency tests were performed and the method was found to work satisfactorily on the Hitachi supercomputer.

Within VISimLab a first but big step was made to couple a supercomputer with the virtual reality environment. This coupling permitted interactions with the computations by adding and removing objects in rooms. The flow computations aimed at efficient ways for computational steering of fluid flow computations. Impressive results have been obtained although some of the results are still demonstrative in nature.

Flows with chemical reactions become important when treating in detail the performance of reactors. In KONWIHR, the metal organic vapour phase epitaxy (MOVPE) was examined in order to support development work on optimising epitaxy methods at various institutes at Bavarian Universities and also in industry. It is shown in the enclosed paper that the AlGaN-growth process could be reliably treated with numerical codes that solve the basic equations of fluid flows and take, in addition, chemical reactions into account.

The project SkvG deals with parallel solution procedures for partial differential equations in order to ensure good performance of computer codes even if large problems are solved. The paper outlines the approach and stresses that the numerical methods used should be based on hierarchical multi-level data and adaptively refined data structure. Space-filling curves are introduced to order the store data in such a way that highly efficient computations can be carried out. This is an approach that justifies new efforts in constructing solvers for partial differential equations for future computations.

As a whole, the projects aiming for fluid flow predictions on supercomputers were successfully completed within KONWIHR and the set of papers presented in this section shows this.

BESTWIHR: Testing of a Closure Assumption for Fully Developed Turbulent Channel Flow with the Aid of a Lattice Boltzmann Simulation

Peter Lammers, Kamen N. Beronov, Thomas Zeiser, and Franz Durst

Institute of Fluid Mechanics
University of Erlangen–Nuremberg
Cauerstraße 4
91058 Erlangen, Germany
{*plammers,kberonov,thzeiser,durst*}*@lstm.uni-erlangen.de*

1 Introduction

The objective in classical turbulence modeling is to construct models for the unknown Reynolds stress tensor in the Reynolds–averaged Navier–Stokes (RANS) equations. One way to do it is to consider the evolution equations for the Reynolds stresses, which can be derived from the original Navier-Stokes equations. In these additional evolution equations, further unknown correlations appear, whose evolution depends in turn on still more unknown correlations. The art of modeling is to a great extent the choice of closure for this infinite system of equations. Here, a closure at the level of the evolution equations for the Reynolds stresses R_{ij} and for their dissipation rate tensor ϵ_{ij} (defined respectively in Eq. (4) and Eq. (8) below) is considered. For all unknown correlations appearing in these evolution equations are modeled, using rational closure assumptions.

To justify a particular closure of this kind, it is necessary to check the approximate validity of these assumptions, at least for some basic flows, such as homogeneous anisotropic incompressible turbulence or developed (time-independent) inhomogeneous turbulence. Reliable databases for all unknown correlations are needed for the selected kinds of turbulent test flows. Since many components of velocity, pressure, and their derivatives are required, such databases are best generated by direct numerical simulation (DNS) of the test flows, because the complete three–dimensional instantaneous flow fields, from which any required statistics can be obtained. This is in many cases not possible with the available measurement techniques like hot-wire anemometry or laser Doppler anemometry.

In spite of the steady increase of computer performance, however, DNS of turbulent flows remains very expensive. Its high memory and CPU time requirements can be met only by supercomputers and only when simulations are restricted to moderate Reynolds numbers. This continues to motivate the development of less ex-

pensive numerical schemes for fluid flow simulation, especially for turbulence. Such schemes must exploit the specific features and advantages of existing and future supercomputers efficiently. The lattice Boltzmann method is a candidate for such a numerical scheme.

This was clearly shown in the work [15] and [16], in which one–point statistics up to higher order were examined. Building on that work, the present paper aims at two goals: First, the lattice Boltzmann results in fully developed plane channel flow are checked, see Sect. 2.1, for the terms, arising in the balance equations of the Reynolds stresses and the dissipation rate, against standard pseudospectral DNS databases. Second, to use lattice Boltzmann simulation to check closure models for the three unknown correlations in the Reynolds stress equations. The esults are presented in Sect. 3.2. The considered closure models are explained in Sect. 2.2.

The computations are done on the Hitachi SR8000–F1 at the Leibniz Rechenzentrum (LRZ) computing center in Munich. The architecture of this computer allows highly flexible programming strategies. Parallelization can be done either by assigning one MPI process to each processor (MPP mode) or in a hybrid way by shared memory parallelization inside one node (SMP mode) and one MPI process on each node. The differences between these two modes are examined in Sect. 3.1, using the computer code $\mathcal{BEST}$ (***B**oltzmann **E**quation **S**olver **T**ool*). This is a 3D lattice Boltzmann solver developed at the authors' institute.

2 Formulation

2.1 The physical problem: fully developed, turbulent, plane channel flow

A test problem for the simulation of turbulence in wall bounded shear flows is the DNS of the so–called minimal channel, a restricted specification [12] based on the well known plane channel flow. The geometry and the used coordinate system are shown in Fig. 1. It is natural to define the Reynolds number by the wall–shear

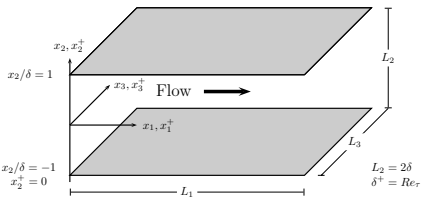

Fig. 1. Computational domain for plane channel flow and coordinate system.

velocity u_τ. From the momentum equation the dependence on the pressure gradient in streamwise direction $\partial p/\partial x_1$ is derived according to

$$u_\tau = \sqrt{\frac{\tau_w}{\rho}} = \sqrt{\frac{\delta}{\rho}\frac{\partial p}{\partial x_1}}, \tag{1}$$

with δ being the channel half-width, ρ the fluid density, and τ_w the wall shear stress. All lengths can then be measured in the "wall units" of velocity length, ,u_τ and ν/u_τ, and are indicated by a $^+$ superscript, as usual. A corresponding Reynolds number can be defined,

$$Re_\tau = \delta u_\tau/\nu = \delta^+ . \tag{2}$$

In order to compare with the databases described in [18] and [23], both of which have

$$Re_\tau = 180 ,$$

the same Re_τ is chosen which for the present DNS, as well. The computations are performed on a grid of $4096{:}256^2$ points, ensuring a uniform spatial resolution of $\Delta x_i^+ \approx 1.4$.

In the simulated flow, the velocity field can be considered periodic in streamwise direction x_1 and in the spanwise direction x_3, provided that the computational grid is large enough to accommodate the correlations lengths in these two direction. The x_1 length must then be especially large. Along the remaining coordinate, the non–slip condition is imposed at the walls, located at $x_2 = \pm\delta$.

It is documented in the literature on DNS of turbulence that a step size of $\Delta = 1.5\eta - 2\eta$, where η is the dissipative (Kolmogorov) length scale, is an upper limit, above which the fine structure of turbulence is not resolved, while $\Delta = \eta$ guarantees full resolution. For the present 2D–channel turbulence, it is estimated [19, exercise 7.8] that $\eta^+ \approx 1.5$ at the wall and η increases with increasing distance from the wall. A uniform grid step size $\Delta^+ \approx 1.5$ in wall units would therefore guarantee a fully resolved DNS, which is the case for the present simulation.

As initial condition, a superposition of an approximation to the expected turbulent mean velocity profile and of streamwise and spanwise vortices is taken. The simulation is continued until $100\,\tau$, before the averaging is started. The time unit $\tau = \delta/u_\tau$ is a physical measure of convective transport by the mean flow. According to experience, initial transients last typically $30\,\tau$, so that the turbulence used for computing the statistics reported below can be considered fully developed indeed. All statistics are obtained by averaging over the $x_1 - x_3$ plane and additionally in time.

2.2 The turbulence model: a Reynolds–stress closure

By introducing the Reynolds decomposition for the velocity and pressure fields,

$$u_i = \overline{u}_i + u_i' , \quad p = \overline{p} + p' ,$$

into the governing incompressible Navier–Stokes equations, one can obtain equations (RANS) for the mean fields $\overline{u}_i, \overline{p}$ and for the disturbances u_i', p'. In the RANS–equations, the so-called Reynolds stress tensor, which is the average of the second–order, one-point moments of fluctuating velocity u_i', is unknown. Often, further equations are taken into account to relegate the closure problem from the level of the RANS to the higher level of equations for the Reynolds stresses themselves and other related second–order moments. This approach was first put forward in [13].

By manipulating the equation for the disturbances, a transport equation for the Reynolds stresses is obtained (see [9] for example):

$$DR_{ij}/Dt = P_{ij} + T_{ij} - 2\epsilon_{ij} + \Pi_{ij} + D_{ij} \tag{3}$$

The following physical meanings are assigned to the tensors in this equation [5]:

$$R_{ij} = \overline{u_i' u_j'} \qquad \text{Reynolds stress component} \tag{4}$$

$$D\overline{u_i' u_j'}/Dt = \partial_t \overline{u_i' u_j'} + \overline{u}_k \partial_k \overline{u_i' u_j'} : \qquad \text{Total change in Reynolds stress} \tag{5}$$

$$P_{ij} = -(\overline{u_j' u_k'} \partial_k \overline{u}_i + \overline{u_i' u_k'} \partial_k \overline{u}_j) : \qquad \text{Production} \tag{6}$$

$$T_{ij} = -\partial_k \overline{u_i' u_j' u_k'} : \qquad \text{Third order velocity correlation, turbulent transport} \tag{7}$$

$$\epsilon_{ij} = \nu \overline{\partial_k u_i' \cdot \partial_k u_j'} : \qquad \text{Dissipation} \tag{8}$$

$$\Pi_{ij} = -\frac{1}{\rho} \left(\overline{u_i' \partial_j p'} + \overline{u_j' \partial_i p'} \right) : \qquad \text{Velocity/pressure gradient correlation} \tag{9}$$

$$D_{ij} = \nu \partial_k^2 \overline{u_i' u_j'} : \qquad \text{Viscous diffusion.} \tag{10}$$

Obviously, the three correlations T_{ij}, Π_{ij}, and ϵ_{ij} are unknown even if the mean flow velocity and pressure were known. By contracting Eq. (5), a similar equation can be obtained for the evolution of the turbulent kinetic energy

$$k = \frac{q^2}{2} = \frac{\overline{u_i' u_i'}}{2}$$

More complicated is the situation in the case of the transport equation for the full tensor of the turbulent dissipation rate. Even if only its trace is considered, as done in the very popular k-ϵ models, see for example [7], the resulting equation contains even more terms that need to be modeled and are difficult to compute or measure. Most of them are modeled in a simple–fashioned way in the two–equation (k-ϵ, k-ω, etc.) models. Here, this equation is written out in its full form:

$$D\epsilon/Dt = P_\epsilon^1 + P_\epsilon^2 + P_\epsilon^3 + P_\epsilon^4 + T_\epsilon + \Pi_\epsilon - \gamma + D_\epsilon . \tag{11}$$

with following definitions of the individual terms (see [21]):

$$D\epsilon/Dt = \partial_t \epsilon + \overline{u}_k \partial_k \epsilon : \qquad \text{Total change in dissipation} \tag{12}$$

$$\begin{aligned} P_\epsilon^1 &= -2\epsilon_{ik} \partial_k \overline{u}_i \\ &= -2\nu \overline{\partial_l u_i' \cdot \partial_l u_k'} \partial_k \overline{u}_i \end{aligned} \qquad \text{Production due to mean velocity gradient} \tag{13}$$

$$\begin{aligned} P_\epsilon^2 &= -2\tilde{\epsilon}_{lk} \partial_l \overline{u}_k \\ &= -2\nu \overline{\partial_l u_i' \cdot \partial_k u_i'} \partial_l \overline{u}_k \end{aligned} \qquad \text{Production due to mean velocity gradient} \tag{14}$$

$$P_\epsilon^3 = -2\nu\overline{u_k' \partial_l u_i'} \cdot \partial_l \partial_k \overline{u}_i : \quad \text{Production due to mixed effects of the gradients of mean and fluctuating velocities (mixed production)} \tag{15}$$

$$P_\epsilon^4 = -2\nu\overline{\partial_l u_i' \cdot \partial_k u_i' \cdot \partial_l u_k'} : \quad \text{Production due to deformation of the vortices (vortex stretching)} \tag{16}$$

$$T_\epsilon = -\nu\partial_k\overline{(u_k' \partial_l u_i' \cdot \partial_l u_i')} \quad \text{Diffusive transport due to turbulent fluctuations} \tag{17}$$

$$\Pi_\epsilon = -\tfrac{2\nu}{\rho}\overline{\partial_l u_i' \partial_i \partial_l p'} : \quad \text{Diffusive transport due to turbulent pressure fluctuations} \tag{18}$$

$$-\gamma = -2\nu^2\overline{(\partial_k \partial_l u_i')^2} : \quad \text{Viscous destruction} \tag{19}$$

$$D_\epsilon = \nu\partial_k^2 \epsilon : \quad \text{Viscous diffusion} \tag{20}$$

In Eq. (11), seven terms are unknown: P_ϵ^1, P_ϵ^2, P_ϵ^3, P_ϵ^4, T_ϵ, Π_ϵ, and γ.

In order to close the equations for the Reynolds stresses, the kinetic turbulent energy and the dissipation rate, the unknown correlations appearing on the right–hand sides of the corresponding evolution equations must be expressed in terms of $\overline{u}_i$ and $\overline{u_i' u_j'}$. In this paper, the lattice Boltzmann DNS results will be used to check closure models for the three correlations of Eq. (5), following the model described in detail in [10]. In particular, reliable modeling of the dissipation rate is needed. As shown by [14], the dissipation can be decomposed according to

$$\epsilon_{ij} = \epsilon_{ij}^h + \epsilon_{ij}^{inh} = -\nu\Delta_\xi(\overline{u_i' u_j''})_0 + \tfrac{1}{4}D_{ij}. \tag{21}$$

Here $\overline{u_i' u_j''}$ is a twopoint correlation in the limit of zero separation in space, $\boldsymbol{\xi} = 0$. For the model itself it is therefore reasonable to solve an equation for the homogeneous part ϵ_h of the ϵ instead of Eq. (11). To elaborate Eq. (21) further, use is made of the observation that for axisymmetric disturbances all involved tensors of rank two are linearly ligned [11]. For example,

$$e_{ij} = \frac{\epsilon_{ij}^h}{\epsilon^h} - \frac{1}{3}\delta_{ij} = A a_{ij} = A\left(\frac{\overline{u_i' u_j'}}{q^2} - \frac{1}{3}\delta_{ij}\right). \tag{22}$$

The tensor a_{ij} is the anisotropy tensor, introduced first by [17]. Combining the above relations, one may write for the case of axisymmetric turbulence

$$\epsilon_{ij} \approx A\epsilon_h a_{ij} + \tfrac{1}{3}\epsilon_h \delta_{ij}. + \tfrac{1}{4}D_{ij}. \tag{23}$$

The function A can depend only on the invariants II_a and II_e of the respective tensors,

$$A = A(II_a, II_e) = \sqrt{II_a / II_e}$$

or alternatively,

$$A = A(II_a, III_a, Re_\lambda) = 1 - J(W - 1), \tag{24}$$

with

$$W(Re_\lambda) = 0.626\left(-0.049Re_\lambda + \tfrac{1}{2}\sqrt{0.009604Re_\lambda^2 + 10.208}\right) \tag{25}$$

and

$$J(II_a, III_a) = 1 - 9\left(\frac{1}{2}II_a - III_a\right), \tag{26}$$

where $Re_\lambda = \lambda q/\nu$ is the Taylor microscale Reynolds number. The Taylor microscale λ itself is defined as $\lambda = \sqrt{5\nu q^2/\epsilon_h}$.

The velocity/pressure–gradient correlation can be split into two parts traditionally called "slow" and "fast" part. Coming from an analytical expression by Chou [5] for homogeneous turbulence, and exact solution for initially-isotropic is given in [6] for turbulence exposed to rapid distortion:

$$\Pi_{ij} = \frac{2}{5}q^2 S_{ij}, \quad II_a \to 0. \tag{27}$$

¿From the dynamic equation of the anisotropy tensor, conclusions are drawn for the behavior of Π_{ij} in two–component turbulence and in decaying, homogeneous, axisymmetric turbulence. Taking the concept of realizability introduced in [22] into account, the following model can be derived,

$$\Pi_{ij} \approx \underbrace{a_{ij}P_{ss} + F\left(\tfrac{1}{3}P_{ss}\delta_{ij} - P_{ij}\right)}_{\Pi_{ij}^{fast}} + \underbrace{C\epsilon_h a_{ij}}_{\Pi_{ij}^{slow}}, \tag{28}$$

with

$$F(II_a, III_a) = \tfrac{3}{5} + \tfrac{18}{5}\left(\tfrac{1}{2}II_a - III_a\right), \tag{29}$$

and

$$C(II_a, III_a, Re_\lambda) = 4.78\,(W-1)\,J. \tag{30}$$

The invariant functions F and C interpolate between the different turbulent states.

The analytical treatment of the turbulent transport correlation T_{ij} is rather difficult because one has to deal with correlation higher than third order in the transport equation for T_{ij}. Supposing once again axisymmetry, the suggested model becomes

$$T_{ij} = c_q \partial_l \frac{\overline{u_i' u_j'}}{q^2}\frac{k^2}{\epsilon_h} J \partial_l k^2 \quad \text{with} \quad c_q = 0.5. \tag{31}$$

This is supposed to be an acceptable approximation only if the transport term is small.

2.3 The numerical method: 3D lattice Boltzmann

The numerical method for the present simulation utilizes the fact that the (macroscopic) velocity field $\mathbf{u}$ and the pressure field p of an viscous fluid can be obtained by solving an kinetic equation for a one–particle, one–point probability density distribution function f, instead of solving the Navier–Stokes equation directly. The function $f = f(\boldsymbol{\xi}, \mathbf{x}, t)$ depends on a microscopic velocity $\boldsymbol{\xi}$, the spatial coordinate $\mathbf{x}$, and the time t. The hydrodynamic fields are given by the moments of the distribution function f. The oldest and best known kinetic equation is the Boltzmann

equation. A radical simplification of that equation and of many other kinetic equations of similar form has been proposed by [1]. This now very popular BGK ansatz for the collision operator is

$$\left(\partial_t + \boldsymbol{\xi} \cdot \boldsymbol{\nabla}_{\mathbf{r}}\right) f(\boldsymbol{\xi}, \mathbf{r}, t) = -\frac{f(\boldsymbol{\xi}, \mathbf{r}, t) - f^{eq}(\boldsymbol{\xi}, \mathbf{r}, t)}{\lambda}. \tag{32}$$

The function f^{eq} is the equilibrium distribution (of Maxwell–Boltzmann kind) and λ is the single parameter of the model, called relaxation time.

The first step to specify a lattice Boltzmann model is the choice of a lattice to discretize the dependence on $\boldsymbol{\xi}$. A finite set of velocities $\mathbf{c}_i$ is chosen. For every $\mathbf{c}_i$ a discrete distribution function f_i is defined. After discretization in space and time, Eq. (32) finally reduces to [4]

$$f_i(\mathbf{x} + \mathbf{c}_i, t + 1) - f_i(\mathbf{x}, t) = -\omega \left(f_i(\mathbf{x}, t) - f_i^{eq}(\rho, \mathbf{u}, t)\right). \tag{33}$$

Eq. (33) appears as an explicit first–order scheme but is in fact second–order in time. In order to proof the equivalence of Eq. (33) and the Navier–Stokes equations the Chapman–Enskog procedure [3] is applied to Eq. (33). By means of this procedure,

$$f_i^{eq} = t_p \rho \left\{1 + \frac{c_{i_\alpha} u_\alpha}{c_s^2} + \frac{u_\alpha u_\beta}{2c_s^2}\left(\frac{c_{i_\alpha} c_{i_\beta}}{c_s^2} - \delta_{\alpha\beta}\right)\right\} \tag{34}$$

can be shown to be an appropriate procedure to recover approximately the incompressible Navier–Stokes dynamics under the condition that the Mach number $|u/c_s| \ll 1$, where c_s is the speed of sound of the model. The parameters t_p depend on the set of discrete velocities $\mathbf{c}_i$ and can be found by a rational algebraic procedure [20]. For turbulent flows the authors have made good experience with the D3Q19 lattice model which is used for the present simulations, as well. As mentioned above, the hydrodynamic quantities are given by moments of f_i, namely

$$\rho = \sum_{i=0}^{n} f_i, \qquad \rho \mathbf{u} = \sum_{i=0}^{n} \mathbf{c}_i f_i, \qquad p = c_s^2 \rho, \tag{35}$$

with $n = 18$ and $c_s^2 = 1/3$ for the chosen model. ¿From the Chapman–Enskog procedure also the expression for the viscosity is deduced which comes out to depend on the relaxation parameter ω as follows,

$$\nu = \frac{1}{6}\left(\frac{2}{\omega} - 1\right).$$

In the present simulation a slight modification of Eq. (33) is used, namely the so-called incompressible D3Q19I model [8, 15]. The procedure to add the pressure gradient into Eq. (33) is described in [2]. To ensure no–slip boundary conditions at the solid walls, at $x_2 = \pm\delta$, the so-called bounce-back rule is applied: The density f_i leaving a node along the direction of $\boldsymbol{\xi}_i$ and bound to cross into the solid wall, is returned to the same node of departure at the subsequent time step as the density associated with the opposite discrete velocity $-\boldsymbol{\xi}_i$.

3 Results

3.1 Hitachi SR8000-F1: MPP versus SMP mode

With the SR8000-series the Japanese vendor of high performance computers Hitachi intended to bring together its MPP architecture SR2201 and its vector architecture S-3000. The final installation at the Leibniz Rechenzentrum consists of 1344 superscalar RISC CPU's with 1.5 Gflops (Giga ***flo**ating **p**oint **op**erations per **s**econd*) peak performance. Each CPU possesses 128 KByte L1–Cache und 160 floating point register . The instruction set allows two ways loading data from main memory to the floating point register . Either by direct transfer of a data element from the main memory to the floating point register (preload) or via prefetch of complete cache lines to the cache followed by a load to the floating point register (prefetch). This second mechanism is used by the compiler in $\mathcal{BESTT}$. The procedure of load (from floating point register) + operation + store to memory in combination with preceding prefetch instructions is called PVP (***P**seudo **V**ector **P**rocessing*) by Hitachi. The CPU's are integrated into shared memory node of 6.5 GByte. Each of these SMP (***S**hared **M**emory **P**rocessing*) nodes consists of 8 CPU's. The nodes are connected by a crossbar network with a bandwidth of 770 MByte/s in the case of $\mathcal{BESTT}$[1]. In Fig. 2(a,b) the performance of $\mathcal{BESTT}$ for the MPP (***M**assively **P**arallel **P**rocessing*) mode is measured for a plane channel geometry with a cross-section consisting of 128^2 grid points. The domain decomposition is done in streamwise direction. In all cases the definition of the speedup is

$$\text{Speedup} = \frac{nT(N,1)}{T(nN,n)}, \tag{36}$$

where T is the compute time, N the problem size on one node or one processor respectively and n the number of nodes (processors). For parallel communication, MPI (***M**essage **P**assing **I**nterface*) is employed. In Fig. 2(a) two nodes are benchmarked by three different grid sizes, with 256, 512 and 1024 points in streamwise direction. As expected, performance increases with increasing compute/communication time ratio. The maximum is 20 MLUP/s (mega lattice side updates per second). This is measured for a processor topology in which neighboring domains are located on the same node as far as possible. In the default setting (round robin) the first domain is on node one, the second on node two, the third domain again on node one and so on. Therefore, communication takes place over the network instead of making use of shared memory inside one node. A noticeable loss in performance is the consequence. In Fig. 2(b) the basic grid size on one node is 512×128^2. The speedup is measured up to 64 processors. A significant performance loss can be observed only for the round-robin setting.

Mode parallelization can be done not only using MPP, but also within each node by running shared memory parallelization with eight threads. Hitachi has named this strategy COMPAS (***C**o-**o**perative **M**icro **P**rocessors in single **A**ddress **S**pace*). In this mode, the memory bandwidth is 32 GBytes/s which matches the aggregated single processor bandwidth. For the largest grid the SMP mode is slightly slower than the MPP mode. But it does not show significant sensibility with respect to

[1] The SR8000-F1 offers a special feature which extent the bandwidth to up to 950 MByte/s.

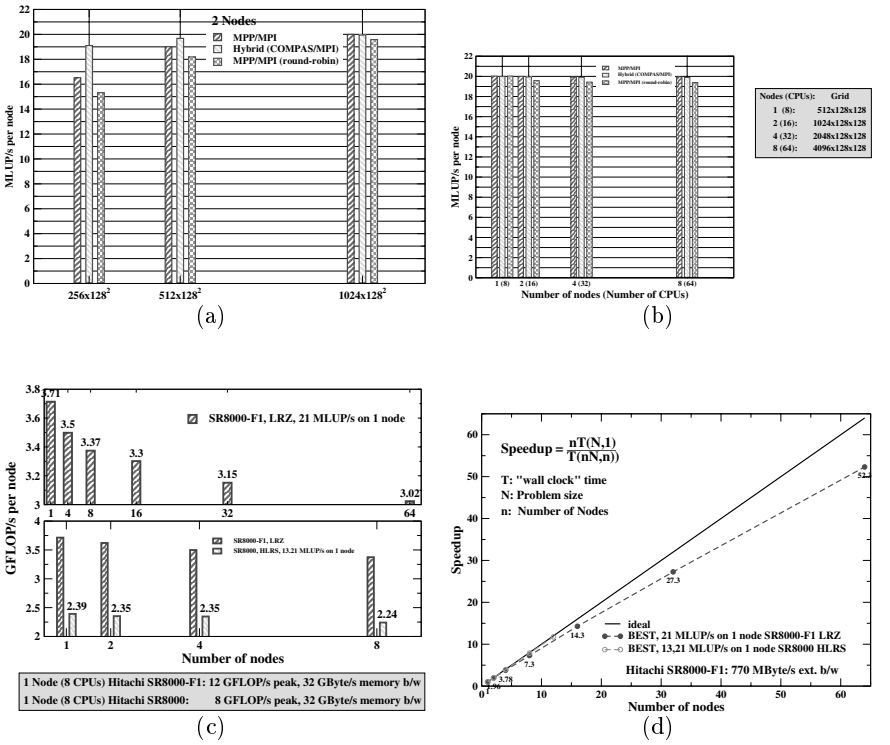

Fig. 2. Performance and speedup of $\mathcal{BEST}$ for Hitachi SR8000-series

grid size. The performance loss between SMP and MPP mode (no round-robin) on the smallest grid is about 14%, as can be seen from Fig. 2(a).

Between the nodes MPI is used again. The communication between the nodes is done by one thread only (hybrid/masteronly). In Fig. 2(c) the machines in Munich with a clock frequency of 350 MHz and in Stuttgart with 250 MHz are compared. Both machines have the same memory bandwidth. The compiler is able to crudely estimate the performance of loop constructs. For the most time consuming loop this information reveals that four floating point operations per load operation should be possible. Therefore $\mathcal{BEST}$ is not limited by the memory bandwidth excessively and should benefit from a higher frequency which is indeed the case[2]. Finally, Fig. 2(d) shows the speedup measurement up to 64 nodes. The SMP mode is used inside the nodes.

[2] The measurements on the SR8000-F1 are done with an older version of $\mathcal{BEST}$ than that used for measurements on the SR8000 in Stuttgart. In the meantime, some additional subroutine calls which do not pertain to the algorithm itself cause a slight performance loss.

3.2 Tensor balance equations for plane channel flow

DNS databases can be used to check turbulent model assumptions as it is shown in the following with the database of the present lattice Boltzmann simulation for the plane channel flow and the model explained in Sect. 2.2. First the results for Eq. (3) and Eq. (11) are validated against the pseudospectral simulations of [18] and [23]. The last simulation uses 256^3 points for the same extensions of the computational domain as in [18], resulting in a twice finer spatial resolution.

In Fig. 3 all quantities from Eq. (3) for the $\overline{u_1' u_1'}$–component of the Reynolds stress are plotted. This component is the most important one. All terms vanish in the

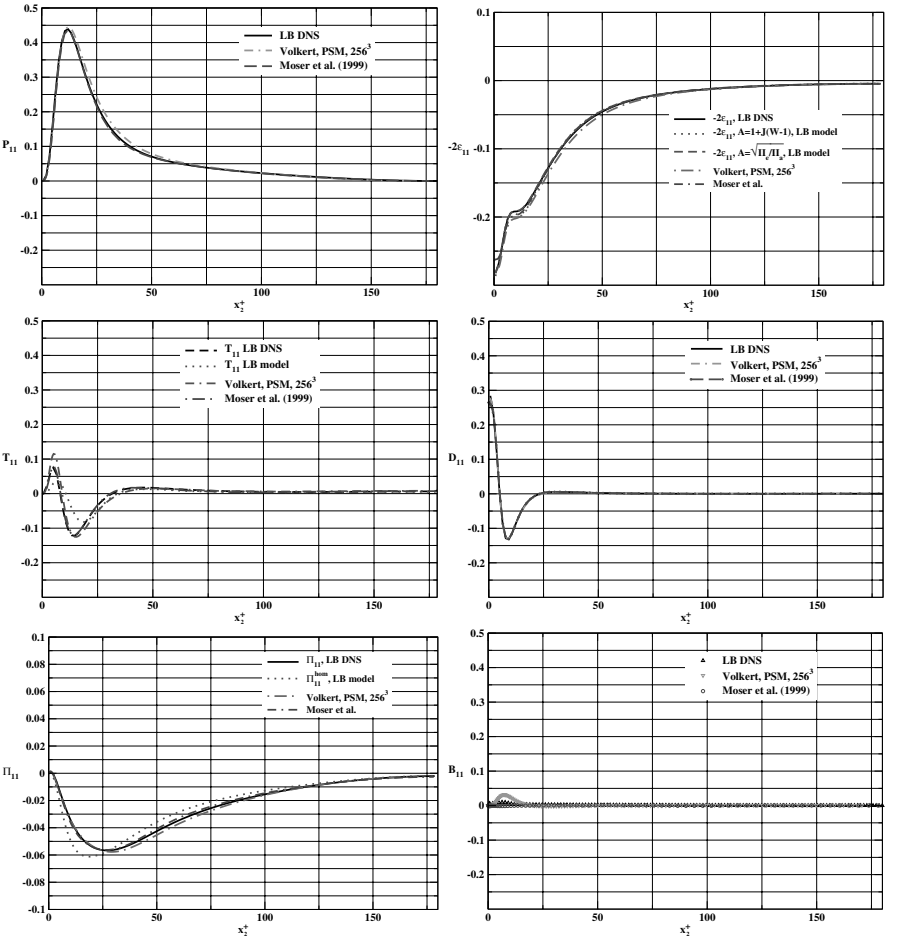

Fig. 3. Comparison of the terms in the balance for $\overline{u_1' u_1'}$, Eq. (3), with the databases [18] und [23]. All terms are scaled with u_τ^4/ν.

center of the channel. Globally, the balance equation for the $\overline{u_1' u_1'}$ component of the

Reynolds stress tensor is clearly dominated by the production and the dissipation term. The largest contribution of the turbulent production by the mean velocity gradient takes place in the buffer layer. Near the wall production becomes zero and the dissipation -2ϵ reaches its minimum. Here the equation is balanced by large viscous diffusion of $\overline{u_1' u_1'}$ from the buffer layer into the viscous sublayer. Inside the buffer layer, the diffusion D_{11} becomes negative. The behavior of the turbulent transport term is similar, except that T_{11} is forced by the boundary conditions to be zero at the wall. The velocity/pressure–gradient correlation influences the balance by a negative contribution reaching the minimum also in the buffer layer. Globally the prediction of the terms is identical for all three simulations. The most significant difference arises for T_{11}. Its extrema in the buffer layer are more distinct in the case of the pseudospectral simulation with finer resolution. But the cross-check of the results done by calculating the balance B_{11} reveals that the balance is not fulfilled so well for this simulation, as it is for the other two simulations.

Along with the DNS results for the individual terms in the balance, the model expressions for the dissipation, the turbulent transport and the velocity/pressure–gradient correlation are plotted in Fig. 3. All modeled correlations vanish in the center of the channel. The model for the dissipation rate ϵ_{11} covers the physics exactly in the whole channel, regardless in which way the function A is obtained. The inhomogeneous part of the dissipation is calculated from the dissipation itself and the viscous diffusion. For T_{11} and Π_{11} the physical behavior is correctly reproduced. Only the extrema are overestimated.

There are three further nontrivial Reynolds stress components, $\overline{u_2' u_2'}$, $\overline{u_3' u_3'}$, and $\overline{u_1' u_2'}$. ¿From these we chose $\overline{u_1' u_2'}$ as one further example. The component ϵ_{12} of the dissipation tensor is not so important as the other ones. The equation is dominated by a negative production and a positive velocity/pressure–gradient correlation, both reaching their extrema in the viscous and the buffer layer. Turbulent transport makes also a significant contribution to the balance. The results for Π_{12} from the three independent DNS match each other globally, but not in detail. The same is the case for T_{12}. Again in the viscous buffer layer the balance is not fulfilled for the pseudospectral simulation with the finer resolution. The reasons are the predictions for the turbulent transport and the velocity/pressure–gradient correlation. Here the extrema are significantly higher (smaller) than in the two other simulations.

The predictive quality of the considered model is very good for the $\overline{u_1' u_2'}$ component, the transport T_{12}, and the velocity/pressure–gradient correlation Π_{12}, whereas the dissipation is predicted poorly. In [24] a model is given, which overcomes this deficiency by taking the stress rate into account.

Finally, the individual terms in Eq. (11) are plotted in Fig. 5. Only the results for the pseudospectral simulation with the higher spatial resolution are used for comparison. At the wall, the balance appears to be dominated by viscous diffusion D_ϵ. But the only term showing a tendency to balance D_ϵ is the destruction term and it is not small enough at the wall. So, the balance is not fulfilled. In comparison with D_ϵ, all others terms are small. Their prediction by both DNS methods is nearly equal, except for the destruction, diffusion and transport terms in a region very close to the wall. For the destruction and diffusion term, the reversal points can not be reproduced with the chosen resolution of the lattice Boltzmann simulation. For T_ϵ, the pseudospectral DNS gives a higher peak near the wall than the lattice Boltzmann DNS.

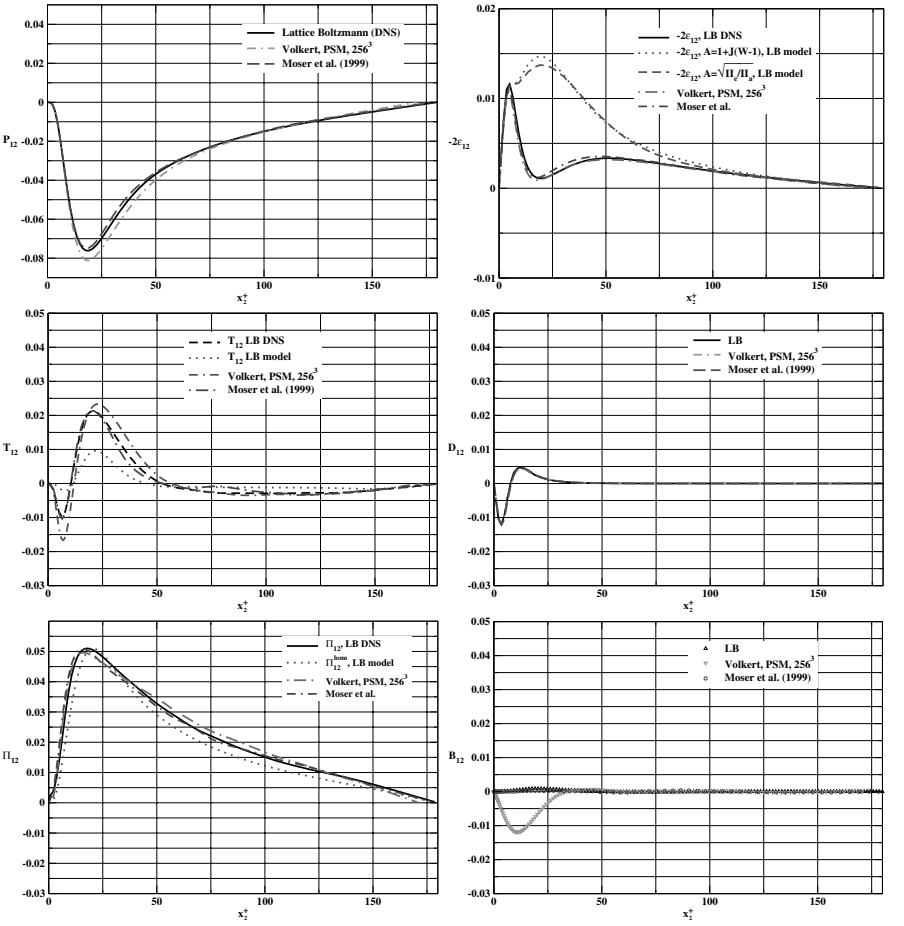

Fig. 4. Comparison of the terms in the balance for $\overline{u_1' u_2'}$, Eq. (3), with the databases [18] and [23]. All terms are scaled with u_τ^4/ν.

4 Summary

A direct numerical simulation (DNS) of developed, turbulent, plane channel flow at a moderate Reynolds number has been performed, using a lattice Boltzmann method. The turbulent flow field is analyzed in terms of detailed contributions to the balance equations for the Reynolds stress tensor and the turbulent dissipation rate tensor components. Generating databases with such statistics is important for turbulence modeling purposes. An example is given in this paper, taking up a model developed at the authors' institute and designed to match the limits of two–component and axisymmetric turbulence, which are important in describing wall–bounded turbulent flows.

The lattice Boltzmann simulation results are obtained in encouraging agreement with earlier DNS using a standard pseudospectral method. The agreement is partic-

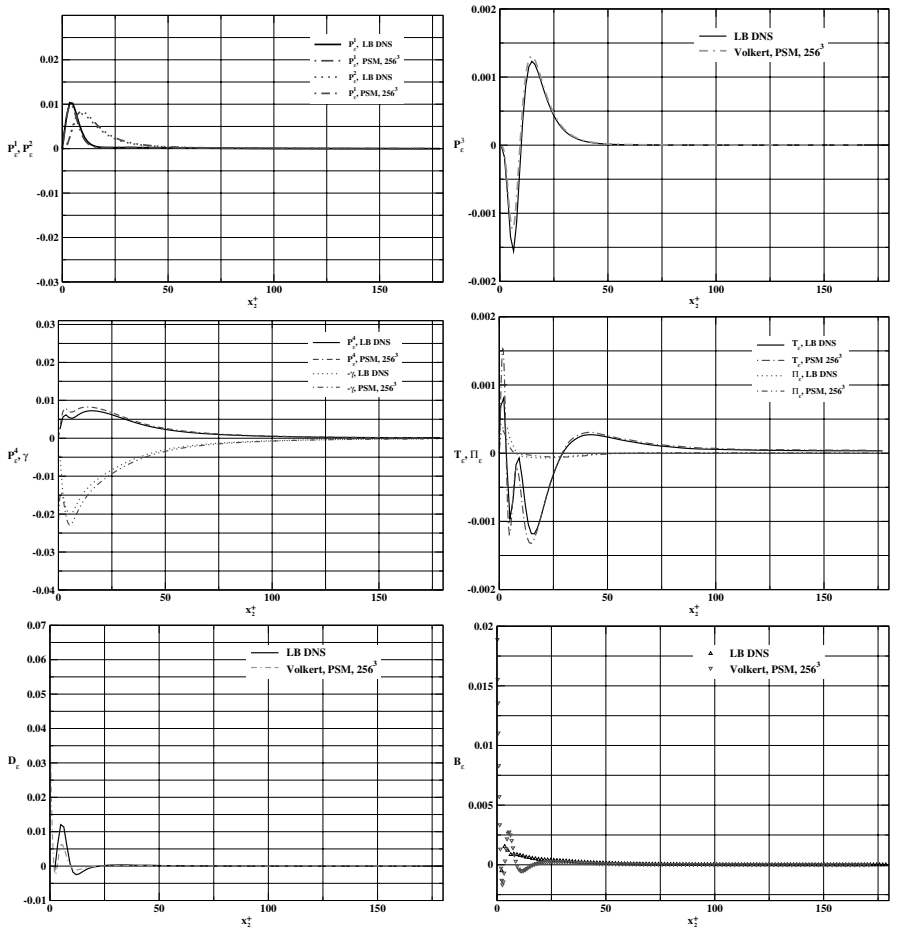

Fig. 5. Comparison of the terms in the balance for ϵ, Eq.(11), with the database [23]. All terms are scaled with u_τ^6/ν^2.

ularly good for the Reynolds stress equations. For the dissipation rate equation, the lattice Boltzmann DNS appears not to have sufficient resolution in the buffer layer in orther to catch some effects present in the most complicated terms of the balance, such as destruction and viscous diffusion of the dissipation rate. Adding a local grid refinement feature to the lattice Boltzmann solver should overcome this problem in general. It may be noted that even the pseudospectral method, which has an inherent strong resolution refinement near the wall and a very high formal precision, experiences problems near the wall, as well. Those with the viscous diffusion term are particularly severe.

With the exception of some benchmarking, all computations have been carried out on the "Bundeshöchstleistungsrechner" computer Hitachi SR8000-F1 at Leibniz Rechenzentrum Munich. This machine can be viewed either as a massively parallel system or as offering a hybrid approach of shared memory nodes connected by a

high capacity crossbar network. Computations based on the former view point use the MPP mode; those based on the latter view point use SMP. With one process in SMP mode, a performance comparable to a vector processor is achieved. For the lattice Boltzmann solver $\mathcal{BEST}$, the same performance can obtained for both modes, globally over a large number of nodes.

In detail, the performance depends on the time ratio of computation to communication. Based on the reported performance measurement results, the MPP mode can be recommended when this ratio is high, and the SMP mode when it is low. This is in accordance with general expectations and shows that the code $\mathcal{BEST}$ allows indeed to use the specifics of the particular parallel architecture.

Acknowledgement. The presented work has been funded by KONWIHR, through the BESTWIHR project and through a grant by the Deutsche Forschungsgemeinschaft. The large–scale computations were carried out at the Leibniz Rechenzentrum. Also gratefully acknowledged is the support by the regional computing center at the University Erlangen–Nuremberg (RRZE), that by the John von Neumann–Institut for Computing (NIC) in Jülich, and that by the computing center at the University Bayreuth. R. Volkert at LSTM has kindly made available some of his data from pseudospectral simulations of channel turbulence at the same Re_τ as for the reported $\mathcal{BEST}$ runs.

References

1. P. Bhatnagar, E. P. Gross, and M. K. Krook. A model for collision processes in gases. I. small amplitude processes in charged and neutral one-component systems. *Phys. Rev.*, 94(3):511–525, 1954.
2. J. Buick and C. Greated. Gravity in lattice Boltzmann model. *Phys. Rev. E*, 61(6):5307–5320, 2000.
3. S. Chapman and T. G. Cowling. *The Mathematical Theory of Non-Uniform Gases.* University Press, Cambridge, 1999.
4. S. Chen and G. D. Doolen. Lattice Boltzmann method for fluid flows. *Annu. Rev. Fluid Mech.*, 30:329–364, 1998.
5. P. Y. Chou. On the velocity correlation and the solution of the equation of turbulent fluctuation. *Q. Appl. Maths.*, 3:38–54, 1945.
6. S. C. Crow. Viscoelastic properties of fine-grained incompressible turbulence. *J. Fluid Mech.*, 33:1–12, 1968.
7. D.C.Wilcox. *Turbulence modelling for CFD.* DCW Industries, Inc., La Cañada, California, 1998.
8. X. He and L.-S. Luo. Lattice Boltzmann model for the incompressible Navier-Stokes equation. *J. Stat. Phys.*, 88(3/4):927–944, 1997.
9. J. O. Hinze. *Turbulence.* McGraw-Hill, New York, 2. edition, 1975.
10. J. Jonanovic. *Konwihr-Vorlesung: Turbulenz und Turbulenzmodellierung II.* Vorlesungsmitschrift, Lehrstuhl für Strömungsmechanik, Universität Erlangen-Nürnberg, 2002.
11. J. Jovanović and I. Otić. On the constitutive relation for the reynolds stresses and the prandtl-kolmogorov hypothesis of effective viscosity in axisymmetric strained turbulence. *Transactions of ASME Journal of Fluids Engineering*, 122:48–50, 2000.

12. J. Kim, P. Moin, and R. Moser. Turbulence statistics in fully developed channel flow at low Reynolds number. *J. Fluid Mech.*, 177, 1987.
13. A. N. Kolmogorov. Equations of motion of an incommpressible turbulent fluid. *Izvestiya Akad Nauk SSSR, Ser. Phys*, 6:56–58, 1942.
14. B. A. Kolovandin and I. A. Vatutin. Statistical transfer theory in non-homogeneous turbulence. *Int. J. Heat Mass Transfer*, 15:2371–2383, 1970.
15. P. Lammers, K. Beronov, G. Brenner, and F. Durst. Direct simulation with the lattice Boltzmann code BEST of developed turbulence in channel flows. In S. Wagner, W. Hanke, A. Bode, and F. Durst, editors, *High Performance Computing in Science and Engineering, Munich 2002*. Springer, 2003.
16. P. Lammers, K. Beronov, R. Volkert, G. Brenner, and F. Durst. Lattice Boltzmann Direct Numerical Simulation of Fully Developed 2d–Channel Turbulence. *Computers & Fluids*, submitted.
17. J. L. Lumley and G. Newman. The return to isotropy of homogeneous turbulence. *J. Fluid Mech.*, 82:161–178, 1977.
18. R. Moser, J. Kim, and N. Mansour. Direct numerical simulation of turbulent channel flow up to $\mathrm{Re}_\tau = 560$. *Phys. Fluids*, 11, 1999.
19. S. B. Pope. *Turbulent Flows*. Cambridge Univ. Press., 2000.
20. Y. H. Qian, D. d'Humières, and P. Lallemand. Lattice BGK models for Navier-Stokes equation. *Europhys. Lett.*, 17(6):479–484, 1992.
21. T. C. Schenk. *Messung der turbulenten Dissipationsrate in ebenen und achsensymmetrischen Nachlaufströmungen*. PhD thesis, Lehrstuhl für Strömungsmechanik, Universität Erlangen-Nürnberg, 1999.
22. U. Schumann. Realizability of Reynolds stress turbulence models. *Phys. Fluids*, 20:721–725, 1977.
23. R. Volkert. *Bestimmung von Turbulenzgrößen zur verbesserten Turbulenzmodellierung auf der Basis von direkten numerischen Simulationen der ebenen Kanalströmung*. PhD thesis, Lehrstuhl für Strömungsmechanik, Universität Erlangen-Nürnberg, 2004. In Vorbereitung.
24. Q.-Y. Ye. *Die turbulente Dissipation mechanischer Energie in Scherschichten*. PhD thesis, Lehrstuhl für Strömungsmechanik, Universität Erlangen-Nürnberg, 1996.

http://www.springer.com/978-3-540-26145-2

High Performance Computing in Science and Engineering, Garching 2004
Transaction of the KONWIHR Result Workshop, October 14-15, 2004, Technical University of Munich, Garching, Germany
Bode, A.; Durst, F. (Eds.)
2005, XI, 301 p., Hardcover
ISBN: 978-3-540-26145-2